

## Supplementary Materials

# 27.20% efficiency for lead-free double perovskite solar cell with all inorganic $\text{Cs}_2\text{BiAgI}_6$ using AZO UTL as a passivation layer

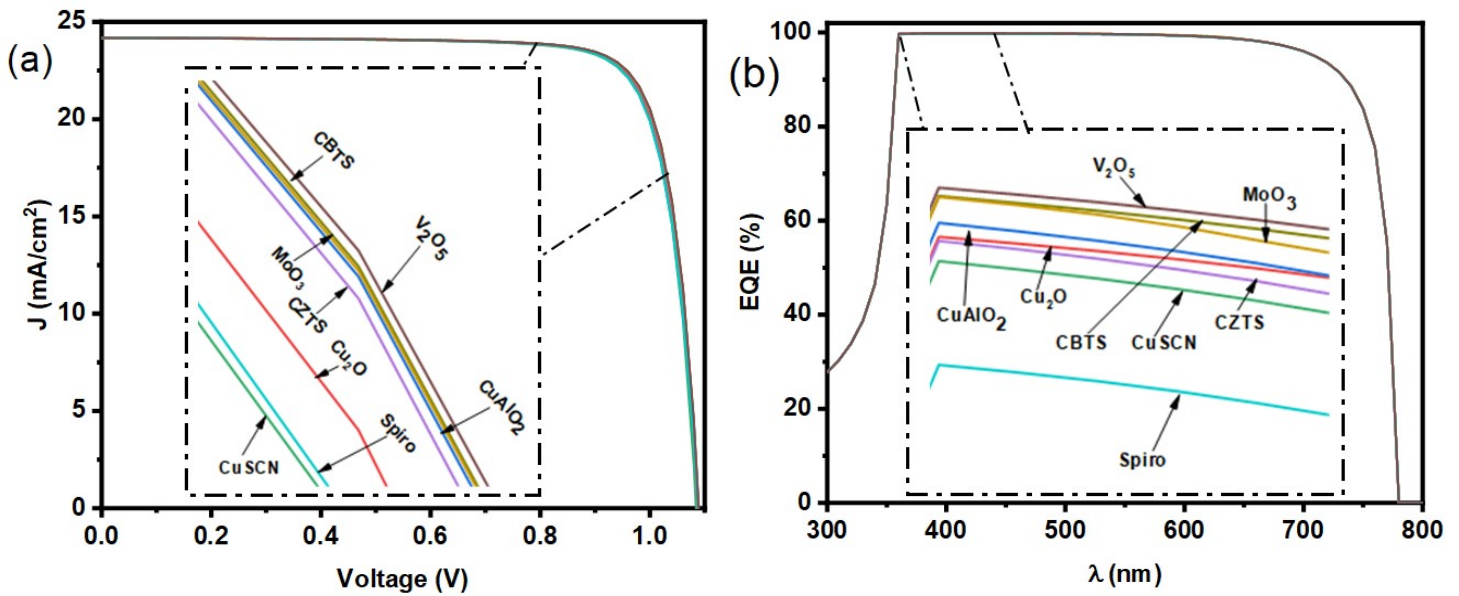
Aminreza Mohandes, Mahmood Moradi, \*<sup>1</sup> 

Department of Physics, College of Science, Shiraz University, 71946-84795 Shiraz, Iran. E-mail: mmoradi@shirazu.ac.ir

CONTENT	Page
Table S1 PV output parameters of 16 devices for two ETLs and eight HTLs material of $\text{Cs}_2\text{BiAgI}_6$ -DPSC, ITO/ETLs/ $\text{Cs}_2\text{BiAgI}_6$ (800 nm)/HTLs/Au	2
Fig. S1 The current density-voltage (J-V) and external quantum efficiency (EQE) curves ((a) and (b)) ZnO/AZO, ((c) and (d)) ZnO. The eight HTLs are shown in the inset of the figures.	3
Fig. S2 Energy band alignment of $\text{Cs}_2\text{BiAgI}_6$ -DPSC (a-h) ZnO/AZO, and (i-p) ZnO.	7
Table S2 Interfacial defect density parameters of ITO/ZnO/AZO/ $\text{Cs}_2\text{BiAgI}_6$ (800 nm)/ $\text{V}_2\text{O}_5$ /Au device	7
Table S3 PV output parameters of simulated $\text{Cs}_2\text{BiAgI}_6$ -DPSC with variation of $\text{VBO}_1$ values, for ITO (500 nm)/ZnO (50 nm)/AZO (10 nm)/ $\text{Cs}_2\text{BiAgI}_6$ (650 nm)/ $\text{V}_2\text{O}_5$ (100 nm)/Au device	8
Fig. S3 (a) J-V curves, (b) energy band diagrams (EBDs), inset of figures demonstrate the variation of energy level of $\text{V}_2\text{O}_5$ -HTL versus $\text{VBO}_1$ values.	8
Table S4 PV output parameters of simulated $\text{Cs}_2\text{BiAgI}_6$ -DPSC with variation of $\text{CBO}_1$ values, for ITO (500 nm)/ZnO (50 nm)/AZO (10 nm)/ $\text{Cs}_2\text{BiAgI}_6$ (650 nm)/ $\text{V}_2\text{O}_5$ (100 nm)/Au device	8
Table S5 PV output parameters of simulated $\text{Cs}_2\text{BiAgI}_6$ -DPSC with variation of $\text{VBO}_2$ values, for ITO (500 nm)/ZnO (50 nm)/AZO (10 nm)/ $\text{Cs}_2\text{BiAgI}_6$ (650 nm)/ $\text{V}_2\text{O}_5$ (100 nm)/Au device	8
Table S6 PV output parameters of simulated $\text{Cs}_2\text{BiAgI}_6$ -DPSC with variation of $\text{CBO}_2$ values, for ITO (500 nm)/ZnO (50 nm)/AZO (10 nm)/ $\text{Cs}_2\text{BiAgI}_6$ (650 nm)/ $\text{V}_2\text{O}_5$ (100 nm)/Au device	9
Fig. S4 (a) J-V curves, (b) energy band diagrams (EBDs), inset of figure shows the alteration energy level of AZO UTL for different values of $\text{CBO}_2$ .	9
Table S7 Comparison of initial and final optimization of PV output parameters of the simulated device for ITO (500 nm)/ZnO (50 nm)/AZO (10 nm)/ $\text{Cs}_2\text{AgBiI}_6$ (650 nm)/ $\text{V}_2\text{O}_5$ (100 nm)/Se device of $\text{Cs}_2\text{AgBiI}_6$ -DPSC	9
Fig. S5 J-V curve of the simulated DPSC, ITO (500 nm)/ZnO (50 nm)/AZO (10 nm)/ $\text{Cs}_2\text{AgBiI}_6$ (650 nm)/ $\text{V}_2\text{O}_5$ (100 nm)/Se device of $\text{Cs}_2\text{AgBiI}_6$ -DPSC, illustrates the initial results and the final results after using the optimized parameters of doping and defect density, energy level, and interfacial defect density.	10

Table S1 PV output parameters of 16 devices for two ETLs and eight HTLs material of  $\text{Cs}_2\text{BiAgI}_6$ -DPSC, ITO/ETLs/ $\text{Cs}_2\text{BiAgI}_6$  (800 nm)/HTLs/Au

No.	Device before optimization	$V_{oc}$ (V)	$J_{sc}$ (mA/cm <sup>2</sup> )	FF (%)	PCE (%)
1	ITO/ZnO/AZO/Cs <sub>2</sub> BiAgI <sub>6</sub> /CBTS/Au	1.0893	24.18	81.89	21.57
2	ITO/ZnO/AZO/Cs <sub>2</sub> BiAgI <sub>6</sub> /Cu <sub>2</sub> O/Au	1.0864	24.17	81.62	21.44
3	ITO/ZnO/AZO/Cs <sub>2</sub> BiAgI <sub>6</sub> /CuAlO <sub>2</sub> /Au	1.0899	24.17	81.84	21.56
4	ITO/ZnO/AZO/Cs <sub>2</sub> BiAgI <sub>6</sub> /CuScN/Au	1.0847	24.16	81.43	21.35
5	ITO/ZnO/AZO/Cs <sub>2</sub> BiAgI <sub>6</sub> /CZTS/Au	1.0883	24.17	81.90	21.55
6	ITO/ZnO/AZO/Cs <sub>2</sub> BiAgI <sub>6</sub> /MoO <sub>3</sub> /Au	1.0894	24.17	81.90	21.57
7	ITO/ZnO/AZO/Cs <sub>2</sub> BiAgI <sub>6</sub> /Spiro/Au	1.0887	24.17	81.21	21.37
8	ITO/ZnO/AZO/Cs <sub>2</sub> BiAgI <sub>6</sub> /V <sub>2</sub> O <sub>5</sub> /Au	1.0897	24.17	81.93	21.59
9	ITO/ZnO/Cs <sub>2</sub> BiAgI <sub>6</sub> /CBTS/Au	1.0890	24.18	81.87	21.56
10	ITO/ZnO/Cs <sub>2</sub> BiAgI <sub>6</sub> /Cu <sub>2</sub> O/Au	1.0862	24.17	81.60	21.43
11	ITO/ZnO/Cs <sub>2</sub> BiAgI <sub>6</sub> /CuAlO <sub>2</sub> /Au	1.0896	24.17	81.82	21.55
12	ITO/ZnO/Cs <sub>2</sub> BiAgI <sub>6</sub> /CuScN/Au	1.0845	24.17	81.41	21.34
13	ITO/ZnO/Cs <sub>2</sub> BiAgI <sub>6</sub> /CZTS/Au	1.0881	24.17	81.88	21.54
14	ITO/ZnO/Cs <sub>2</sub> BiAgI <sub>6</sub> /MoO <sub>3</sub> /Au	1.0891	24.17	81.87	21.56
15	ITO/ZnO/Cs <sub>2</sub> BiAgI <sub>6</sub> /Spiro/Au	1.0884	24.17	81.19	21.36
16	ITO/ZnO/Cs <sub>2</sub> BiAgI <sub>6</sub> /V <sub>2</sub> O <sub>5</sub> /Au	1.0894	24.17	81.91	21.58



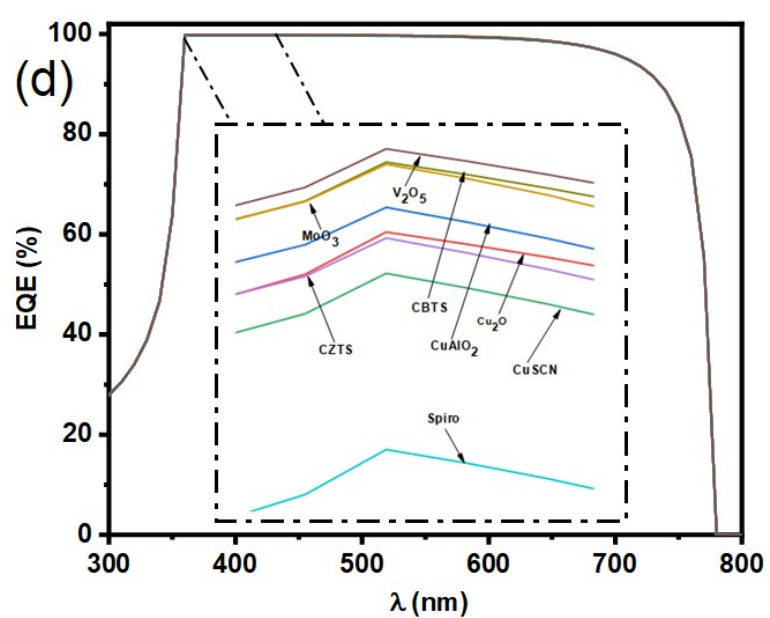
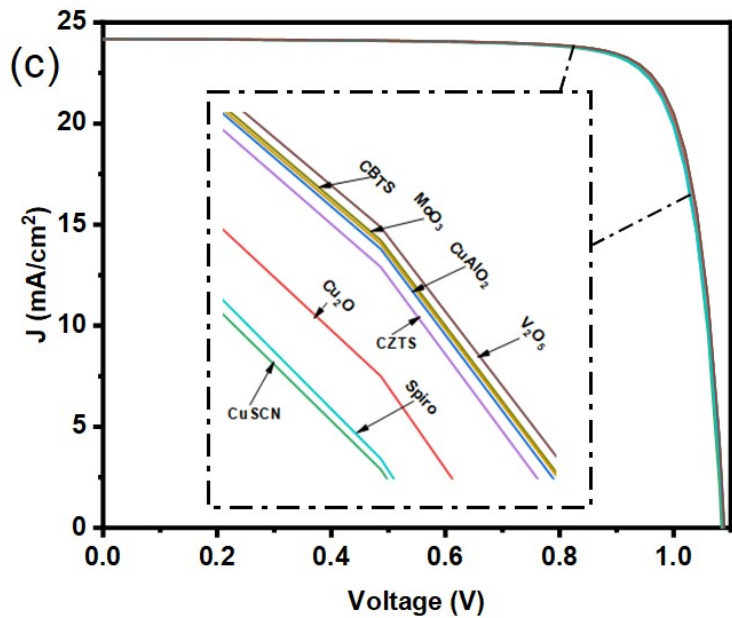
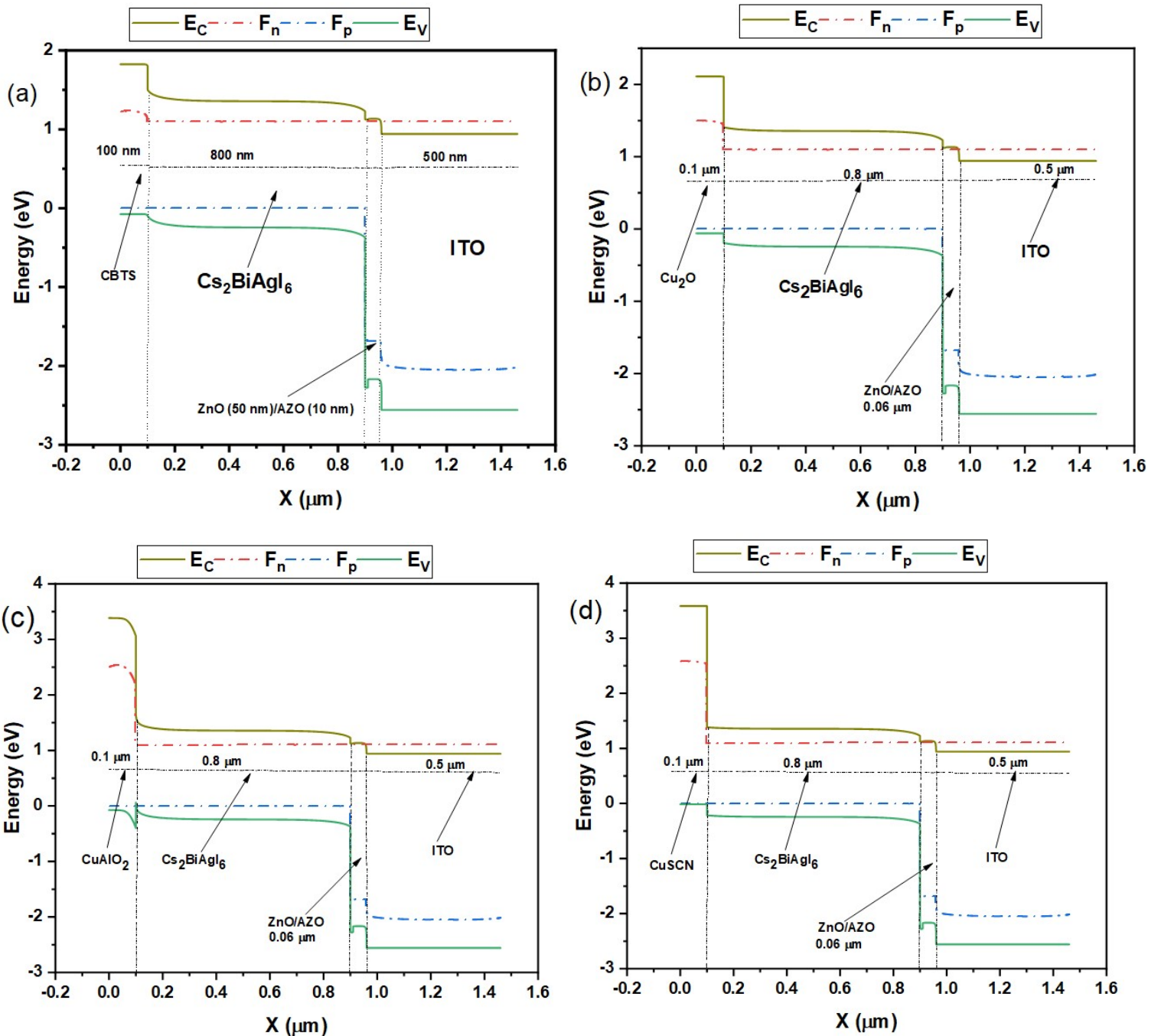
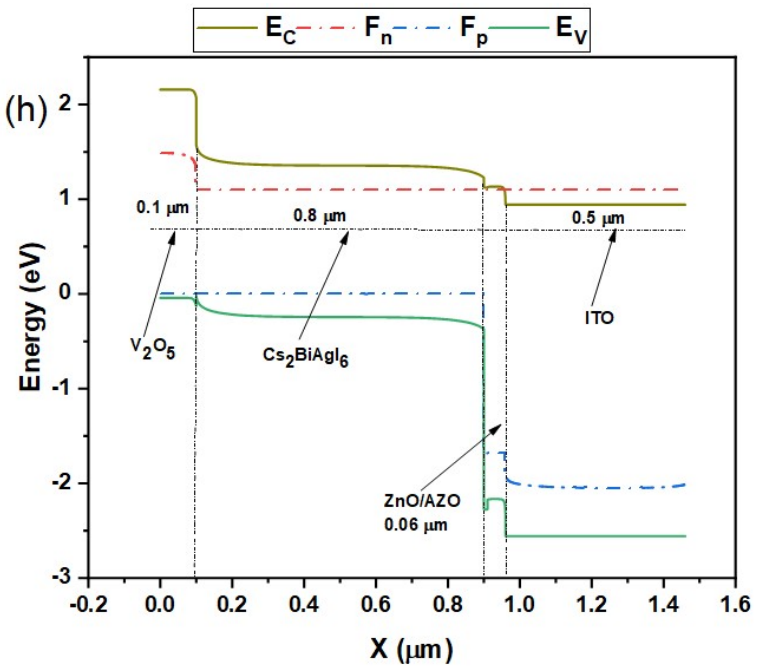
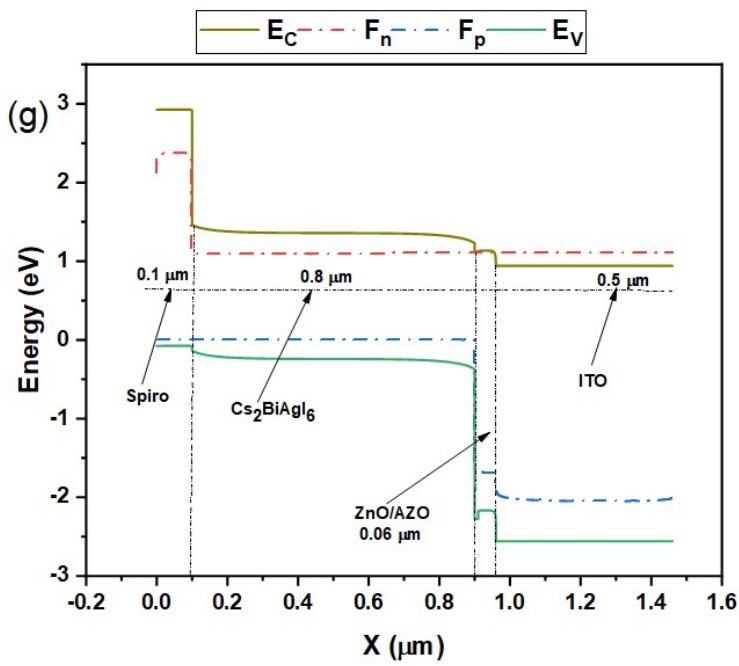
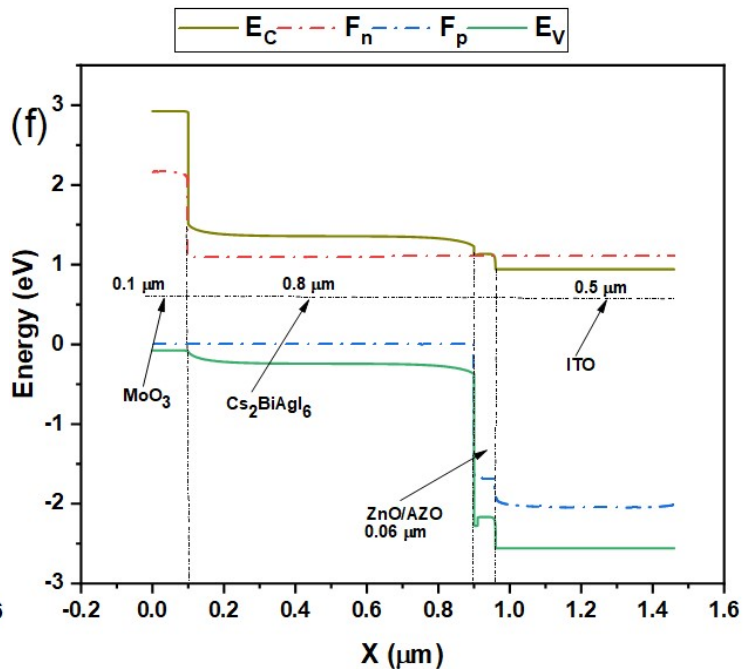
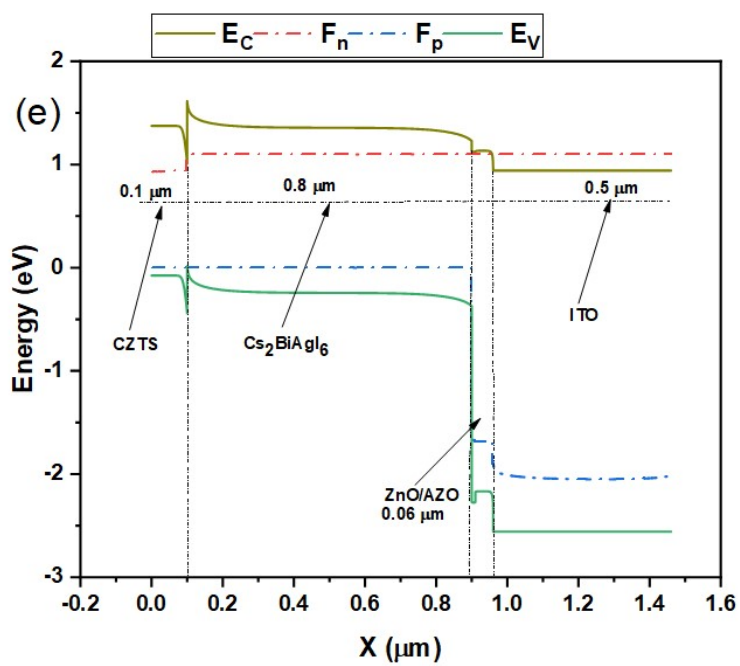
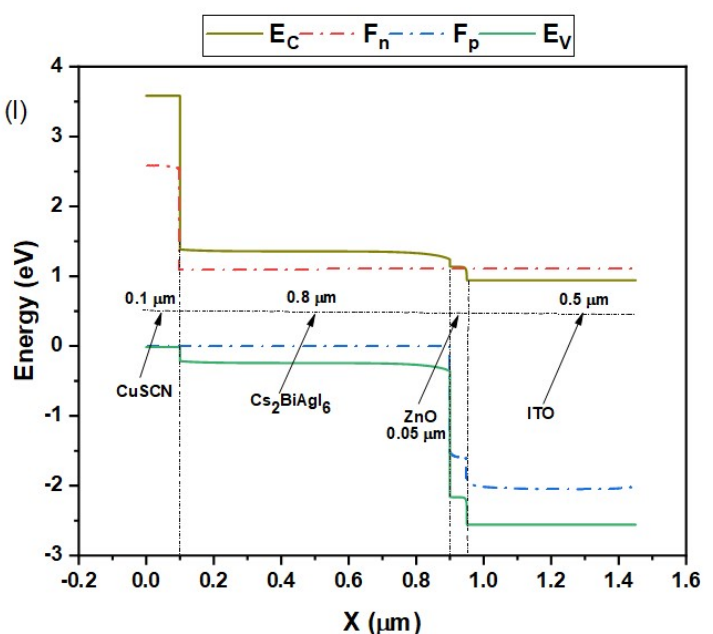
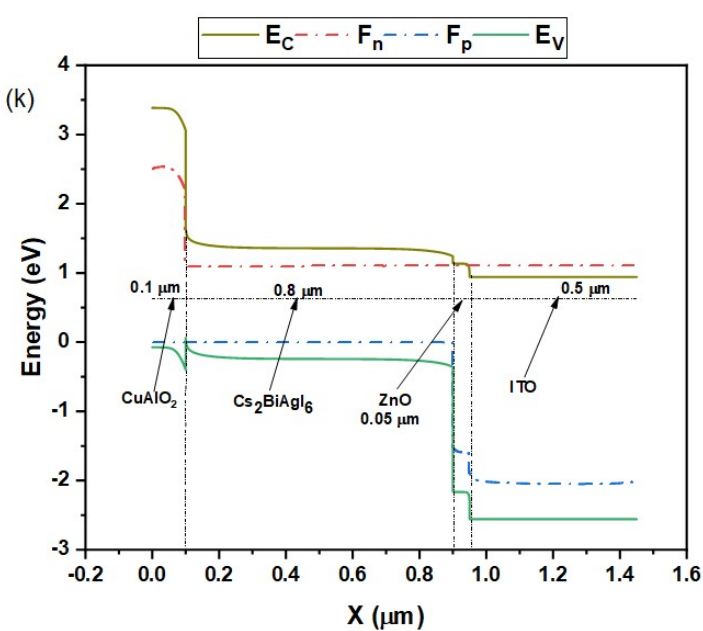
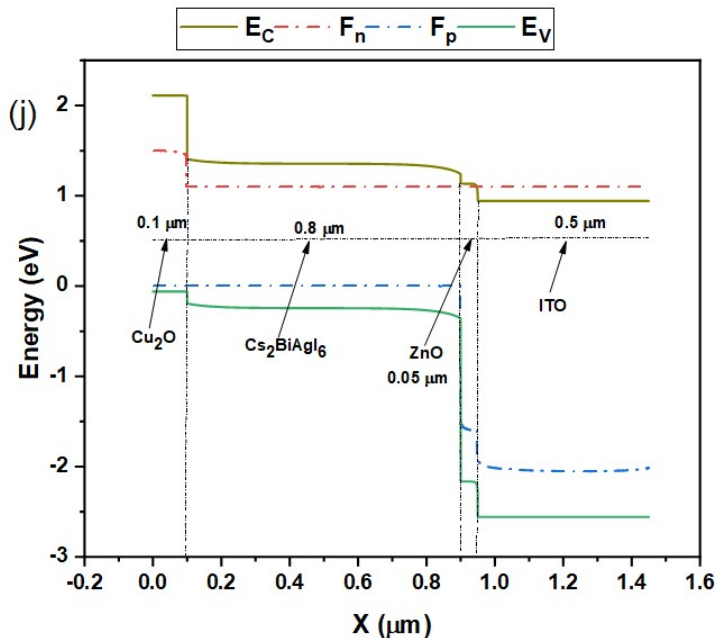
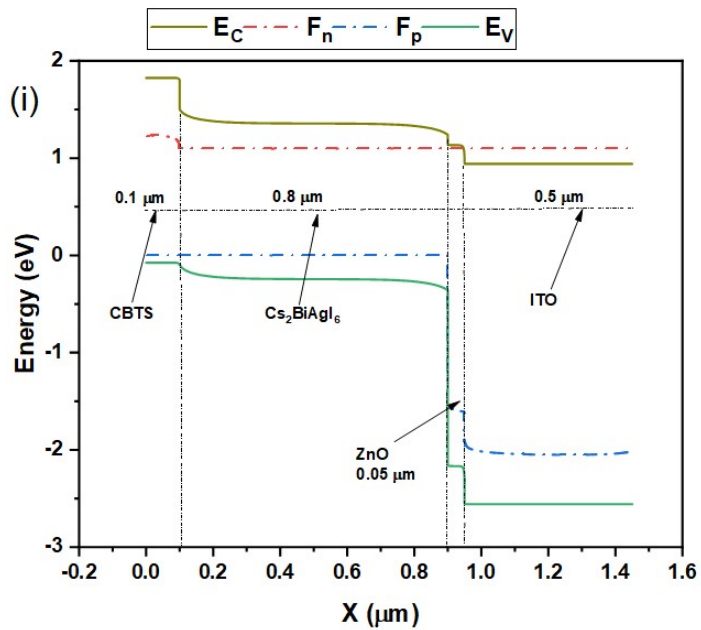


Fig. S1 The current density-voltage (J-V) and external quantum efficiency (EQE) curves (a and b) ZnO/AZO, and (c and d) ZnO. The eight HTLs are shown in the inset of the figures.







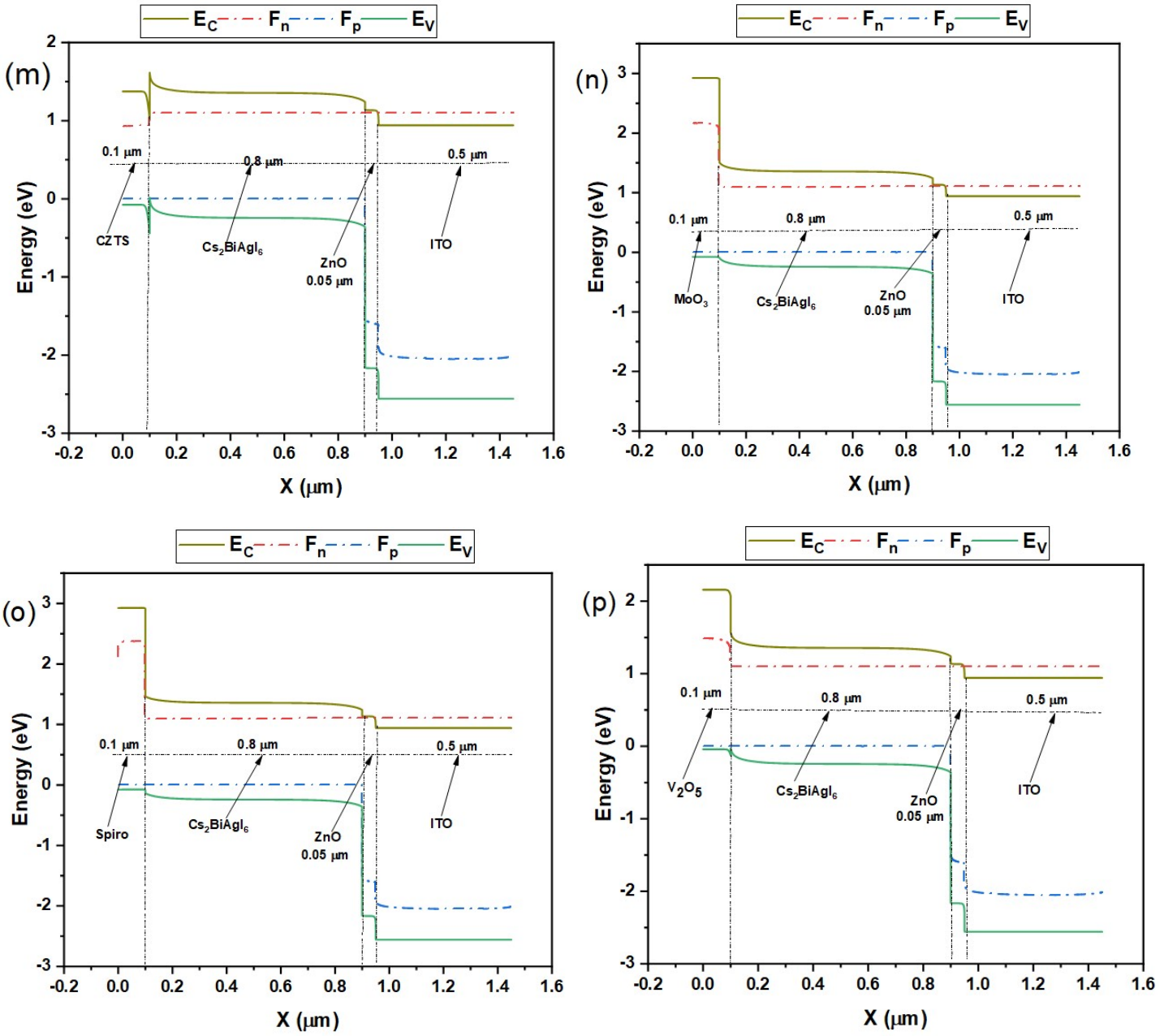


Fig. S2 Energy band alignment of  $\text{Cs}_2\text{BiAgI}_6$ -DPSC (a-h) ZnO/AZO, and (i-p) ZnO. ( $E_C$  (conduction band energy),  $F_n$  (quasi-fermi level of electron energy),  $F_p$  (quasi-fermi level of hole energy), and  $E_V$  (valence band energy)).

Table S2 Interfacial defect density parameters of ITO/ZnO/AZO/ $\text{Cs}_2\text{BiAgI}_6$  (800 nm)/ $\text{V}_2\text{O}_5$ /Au device

Parameter	ZnO/AZO	AZO/ $\text{Cs}_2\text{BiAgI}_6$	$\text{Cs}_2\text{BiAgI}_6/\text{V}_2\text{O}_5$
Defect type	Neutral	Neutral	Neutral
$\sigma_n$ (cm <sup>2</sup> )	$1 \times 10^{-17}$	$1 \times 10^{-17}$	$1 \times 10^{-18}$
$\sigma_p$ (cm <sup>2</sup> )	$1 \times 10^{-18}$	$1 \times 10^{-18}$	$1 \times 10^{-19}$
Distribution of energy	Single	Single	Single
$E_t - E_V$	Above the VB maximum	Above the VB maximum	Above the VB maximum
Energy level w.r.t. Reference (eV)	0.6	0.6	0.6
$N_i$ (cm <sup>-2</sup> )	$1 \times 10^{10}$	$1 \times 10^{10}$	$1 \times 10^{10}$

Table S3 PV output parameters of simulated  $\text{Cs}_2\text{BiAgI}_6$ -DPSC with variation of  $\text{VBO}_1$  values, for ITO (500 nm)/ZnO (50 nm)/AZO (10 nm)/ $\text{Cs}_2\text{BiAgI}_6$  (650 nm)/ $\text{V}_2\text{O}_5$  (100 nm)/Au device

Band gap energy of HTL (eV)	$\text{VBO}_1$ (eV)	Structure type	$V_{oc}$ (V)	$J_{sc}$ ( $\text{mA cm}^{-2}$ )	FF (%)	PCE (%)
1.5	-0.6	Cliff	1.0491	24.40	78.32	20.05
1.6	-0.5	Cliff	1.1462	23.79	79.48	21.68
1.7	-0.4	Cliff	1.2347	23.71	81.29	23.80
1.8	-0.3	Cliff	1.2946	23.85	82.15	25.98
1.9	-0.2	Cliff	1.3146	23.86	86.07	27
2	-0.1	Cliff	1.3193	23.84	86.36	27.17
<b>2.1</b>	<b>0.0</b>	<b>Cliff</b>	<b>1.3210</b>	<b>23.84</b>	<b>86.32</b>	<b>27.19</b>
2.2	+0.1	Spike	1.3213	23.83	86.31	27.18
2.3	+0.2	Spike	1.3213	23.83	86.31	27.18
2.4	+0.3	Spike	1.3213	23.83	86.31	27.18
2.5	+0.4	Spike	1.3214	23.83	86.29	27.17

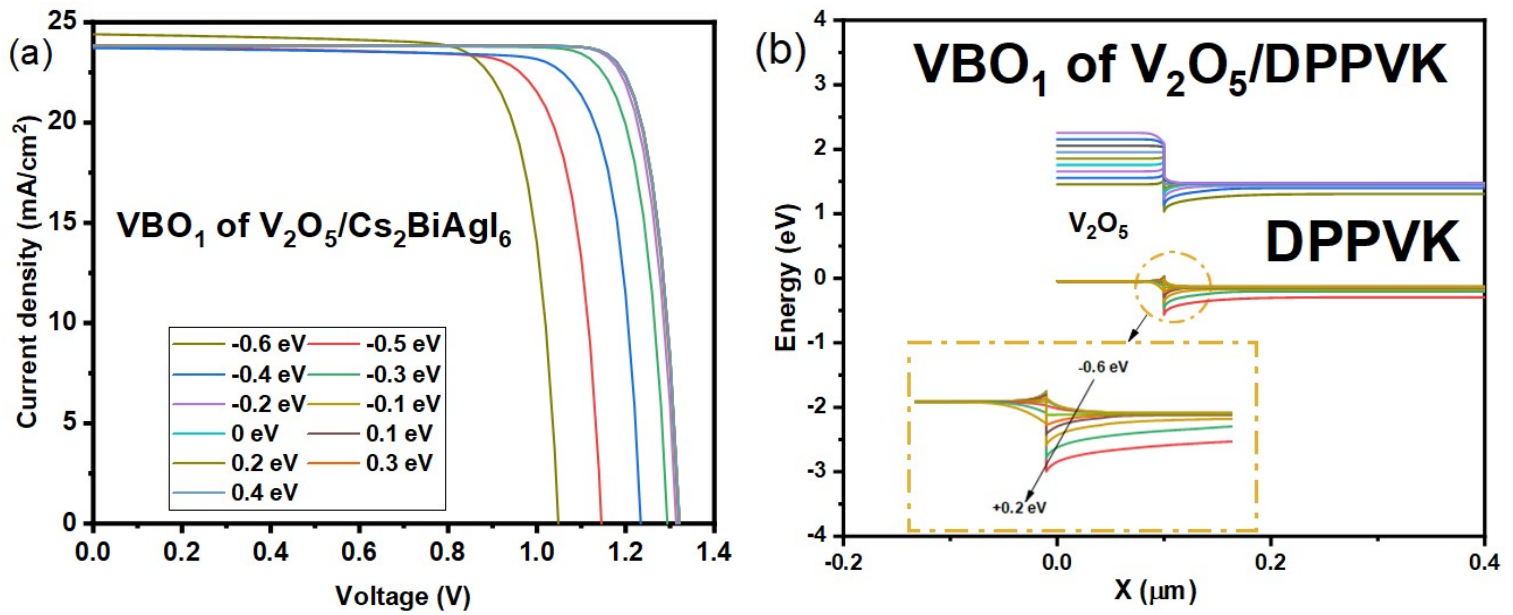


Fig. S3 (a) J-V curves, (b) energy band diagrams (EBDs), inset of figures demonstrate the variation of energy level of  $\text{V}_2\text{O}_5$ -HTL versus  $\text{VBO}_1$  values.

Table S4 PV output parameters of simulated  $\text{Cs}_2\text{BiAgI}_6$ -DPSC with variation of  $\text{CBO}_1$  values, for ITO (500 nm)/ZnO (50 nm)/AZO (10 nm)/ $\text{Cs}_2\text{BiAgI}_6$  (650 nm)/ $\text{V}_2\text{O}_5$  (100 nm)/Au device

Electron affinity of $\text{V}_2\text{O}_5$	$\text{CBO}_1$	$V_{oc}$ (V)	$J_{sc}$ ( $\text{mA cm}^{-2}$ )	FF (%)	PCE (%)
3	0.4	1.2370	23.62	81.11	23.70
3.1	0.3	1.2951	23.80	84.11	25.93
3.2	0.2	1.3146	23.83	86.07	26.97
3.3	0.1	1.3193	23.84	86.36	27.16
<b>3.4</b>	<b>0.0</b>	<b>1.3210</b>	<b>23.84</b>	<b>86.32</b>	<b>27.19</b>
3.5	-0.1	1.3213	23.84	86.31	27.19
3.6	-0.2	1.3213	23.84	86.31	27.19

Table S5 PV output parameters of simulated  $\text{Cs}_2\text{BiAgI}_6$ -DPSC with variation of  $\text{VBO}_2$  values, for ITO (500 nm)/ZnO (50 nm)/AZO (10 nm)/ $\text{Cs}_2\text{BiAgI}_6$  (650 nm)/ $\text{V}_2\text{O}_5$  (100 nm)/Au device

Energy band gap of AZO	$\text{VBO}_2$	$V_{oc}$ (V)	$J_{sc}$ ( $\text{mA cm}^{-2}$ )	FF (%)	PCE (%)
3	-1.5	1.321	23.84	86.32	27.19
3.1	-1.6	1.321	23.84	86.32	27.19
3.2	-1.7	1.321	23.84	86.32	27.19
3.3	-1.8	1.321	23.84	86.32	27.19
<b>3.4</b>	<b>-1.9</b>	<b>1.321</b>	<b>23.84</b>	<b>86.32</b>	<b>27.19</b>
3.5	-2.0	1.321	23.81	86.30	27.14

Table S6 PV output parameters of simulated  $\text{Cs}_2\text{BiAgI}_6$ -DPSC with variation of  $\text{CBO}_2$  values, for ITO (500 nm)/ZnO (50 nm)/AZO (10 nm)/ $\text{Cs}_2\text{BiAgI}_6$  (650 nm)/ $\text{V}_2\text{O}_5$  (100 nm)/Au device

Electron affinity of AZO (eV)	$\text{CBO}_2$ (eV)	Structure Type	$V_{oc}$ (V)	$J_{sc}$ ( $\text{mA cm}^{-2}$ )	FF (%)	PCE (%)
3.5	+0.4	Spike	1.323	23.84	82.10	25.90
3.6	+0.3	Spike	1.3222	23.84	86.15	27.16
3.7	+0.2	Spike	1.3222	23.84	86.28	27.20
3.8	+0.1	Spike	1.3222	23.84	86.28	27.20
<b>3.9</b>	<b>+0.0</b>	<b>Cliff</b>	<b>1.3221</b>	<b>23.84</b>	<b>86.29</b>	<b>27.20</b>
4	-0.1	Cliff	1.321	23.84	86.32	27.19
4.1	-0.2	Cliff	1.3097	23.83	86.94	27.14

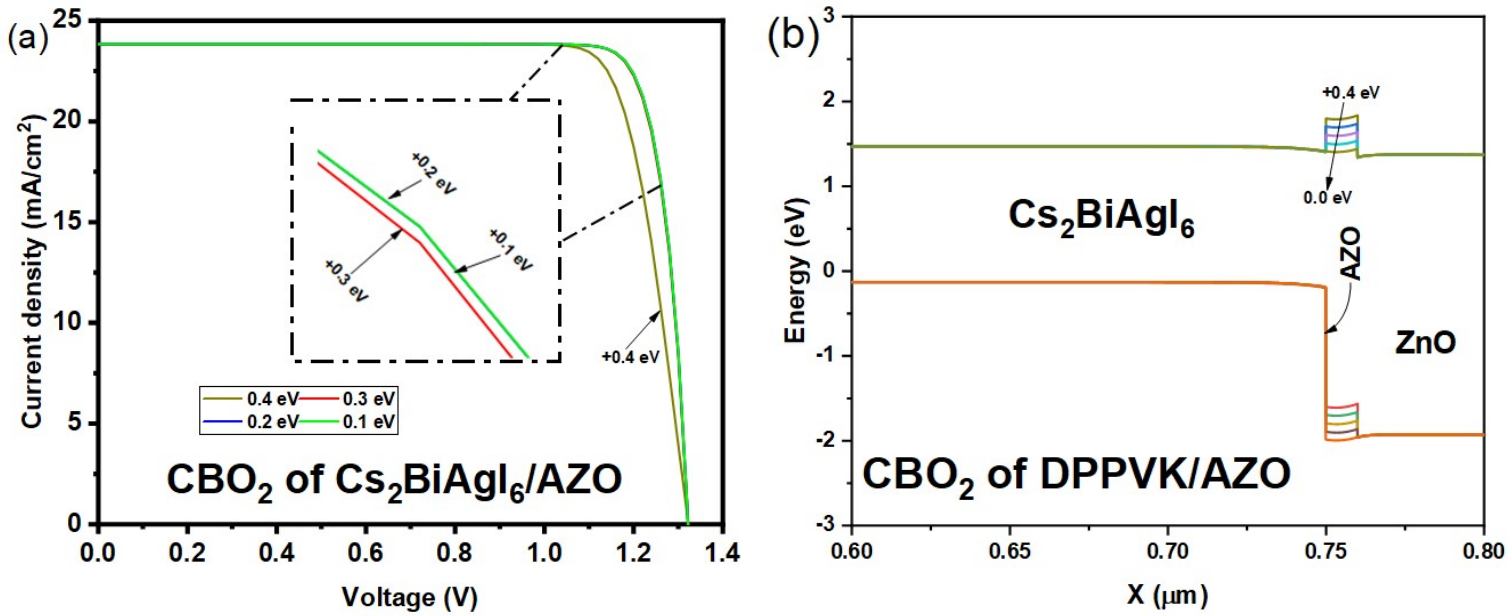


Fig. S4 (a) J-V curves, inset shows affinity variation, (b) energy band diagrams (EBDs) of AZO UTL for different values of  $\text{CBO}_2$ .

Table S7 Comparison of initial and final optimization of PV output parameters of the simulated device for ITO (500 nm)/ZnO (50 nm)/AZO (10 nm)/ $\text{Cs}_2\text{AgBiI}_6$  (650 nm)/ $\text{V}_2\text{O}_5$  (100 nm)/Se device of  $\text{Cs}_2\text{AgBiI}_6$ -DPSC

No.	Parameters of $\text{Cs}_2\text{AgBiI}_6$ -DPSC	$V_{oc}$ (V)	$J_{sc}$ ( $\text{mA cm}^{-2}$ )	FF (%)	PCE (%)
1	Initial parameters (without optimization)	1.1005	23.78	82.78	21.67
2	Doping and Defect density of all layers optimization	1.3212	23.83	86.31	27.17
3	Energy level optimization	1.3221	23.84	86.28	27.20
4	Interfacial defect density optimization (final optimization)	1.3221	23.84	86.28	27.20

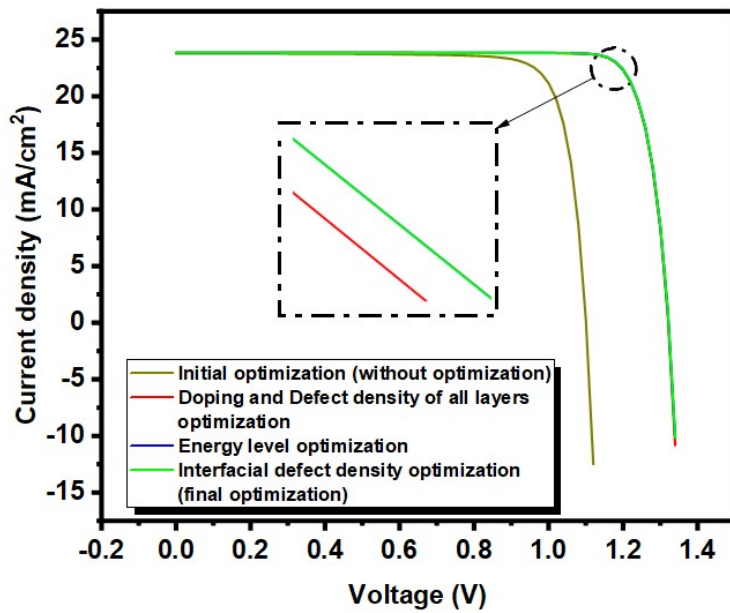


Fig. S5 J-V curve of the simulated DPSC, ITO (500 nm)/ZnO (50 nm)/AZO (10 nm)/Cs<sub>2</sub>AgBi<sub>6</sub> (650 nm)/V<sub>2</sub>O<sub>5</sub> (100 nm)/Se device of Cs<sub>2</sub>AgBi<sub>6</sub>-DPSC, illustrates the initial results and the final results after using the optimized parameters of doping and defect density, energy level, and interfacial defect density.